Showcasing research from Professor Haritz Sardon's laboratory, School of Chemistry, University of Basque Country UPV/EHU, Gipuzkoa, Spain.

Oxime metathesis: tuneable and versatile chemistry for dynamic networks

In this manuscript we explore the use of oxime metathesis as a versatile dynamic network in polymers. We discover that polymers bearing oximes can be reprocessed under acid catalysis while maintaining their structural integrity.

As featured in:

See Haritz Sardon *et al.*,
Chem. Sci., 2024, **15**, 2359.

ROYAL SOCIETY
OF **CHEMISTRY**

rsc.li/chemical-science

EDGE ARTICLE

Check for updates

Oxime metathesis: tuneable and versatile chemistry for dynamic networks†

Luca Pettazzoni,[a] Marta Ximenis, [ID][b] Francesca Leonelli, [ID][a] Giulia Vozzolo,[b] Enrico Bodo, [ID][a] Fermin Elizalde[b] and Haritz Sardon [ID] *[bc]

Oxime chemistry has emerged as a versatile tool for use in a wide range of applications. In particular, the combination of oximes with esters and urethanes has enabled the realisation of Covalent Adaptable Networks (CANs) with improved and tunable dynamic properties. Nevertheless, an exclusively oxime-based chemistry has not yet been explored in the fabrication of CANs. In this work, we investigate the mechanism of the acid-catalysed dynamic exchange of oximes. We propose a metathesis mechanism that is well supported by both experimental and computational studies, which highlight the importance of the substituent effect on the exchange reaction kinetics. Then, as a proof of concept, we incorporate oxime groups into a cross-linked polymeric material and demonstrate the ability of oxime-based polymers to be reprocessed under acid catalysis while maintaining their structural integrity.

Introduction

The term Dynamic Covalent Chemistry (DCC) refers to a variety of reactions that involve covalent bonds that can be cleaved, reformed or exchanged upon a given applied stimulus.[1] This enables the creation of dynamic chemical systems with a wide range of potential applications such as drug delivery, molecular machines, sensors and bioconjugation.[2–4] The introduction of DCC into polymeric materials has led to the development of Covalent Adaptable Networks (CANs),[5,6] which consist of cross-linked structures bound through reversible covalent bonds. The dynamic nature of the cross-linking points allows CANs to be recyclable and reprocessable while keeping thermoset-like mechanical properties.[7,8]

To date, a large variety of dynamic reactions have been explored to produce CANs, including transesterification,[9] transcarbamoylation,[10] disulfide exchange,[11,12] Diels–Alder[13] and imine exchange.[14] Imine chemistry in particular provides a versatile method for the fabrication of dynamic networks.[15] Indeed, imine chemistry has been used to fabricate dynamic networks from the reaction of amines and aldehydes, obtaining

materials that are reshapable and reprocessable.[16,17] However, although the hydrolytic stability of imine bonds has been used advantageously for the development of acid-degradable materials,[18] hydrolysis reactions are often a drawback when it comes to the practical use of these systems.

Oximes have emerged as robust alternatives to imines or the related hydrazones.[19,20] Their enhanced kinetic and thermodynamic stability is attributed to electronic contributions from the delocalisation of the O– lone pair in the C=N bond.[21] For example, direct evidence of the enhanced stability of oximes over imines has been seen in polyethylene glycol-like polymers.[22] Whilst PEG-containing imine linkages suffered rapid hydrolysis in aqueous buffer (pH = 7.4), the analogue PEG-oxime degrades only 25% in 5 days.

Interestingly, the increased hydrolytic stability of oximes has also been used for the preparation of dynamic hydrogels.[23–25] For instance, Sumerlin and coworkers reported oxime-based hydrogels obtained from a statistical keto-functional copolymer of *N,N*-dimethylacrylamide (DMA) and diacetone acrylamide (DAA) reacted with functional alkoxyamines.[24] The resulting hydrogels were self-healable and stimuli-responsive.

In the search for more robust dynamic materials, oximes have appeared in literature in combination with other chemistries. For instance, the combination of oxime-type linkages in ester, urethane and urea chemistries has allowed the preparation of poly(oxime-ester),[26] poly(oxime-urethane)[27] and poly(urea-oxime-urethane).[28] In all cases the introduction of oxime chemistry has allowed the materials to be reprocessed, even without the addition of a catalyst.

It is well-known that imines undergo exchange through three different competing reactions: imine metathesis, transamination and imine formation/hydrolysis (Fig. 1).[29] Due to the

[a]Department of Chemistry, Sapienza Università di Roma, Piazzale Aldo Moro 5, 00185 Rome, Italy

[b]POLYMAT University of the Basque Country UPV/EHU, Joxe Mari Korta Center, Avda. Tolosa 72, 20018 Donostia-San Sebastian, Spain. E-mail: haritz.sardon@ehu.eus

[c]Department of Polymers and Advanced Materials: Physics, Chemistry and Technology, Faculty of Chemistry, University of the Basque Country. UPV/EHU, Donostia-San Sebastián 20018, Spain
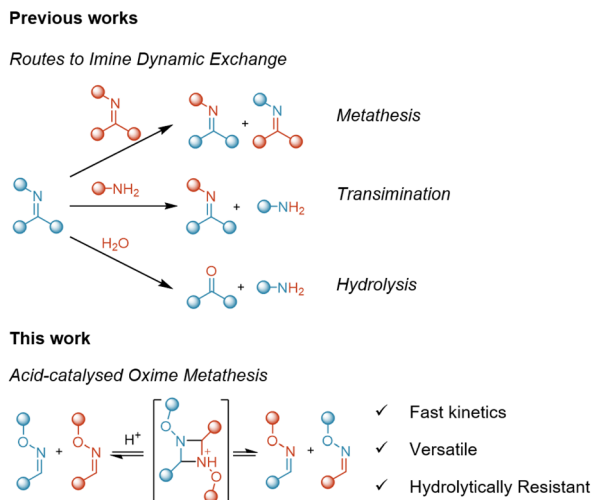
Fig. 1 Imine dynamic exchange mechanisms comprising metathesis, transamination and hydrolysis. Acid-catalysed oxime metathesis reaction presented herein.

similar structural features of imines and oximes, in this work we aim to investigate the metathesis of oximes as a potential dynamic exchange mechanism which can be translated from molecular reactions to polymeric materials. Thus, we will consider equimolar systems relying on pure oximes, without amine or free oxime excess.

Results and discussion

To understand the dynamic behaviour of oximes, we first prepared a representative set of oxime ethers (**3a–3i**, Scheme 1) starting from the corresponding aldehydes **1a–1g** (ESI section, Materials and methods†).

We ran an initial set of reactions exploring the catalyst effect, by choosing oximes **3b** and **3c** as model compounds (Fig. 2b and S1†). The equimolar reaction was conducted in bulk at 100 °C and the progress was followed by ^{1}H-NMR spectroscopy using
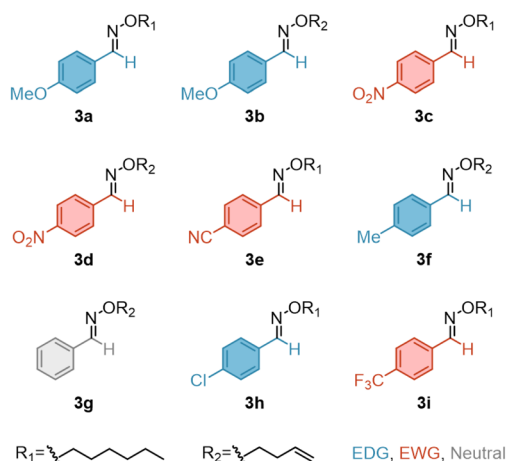
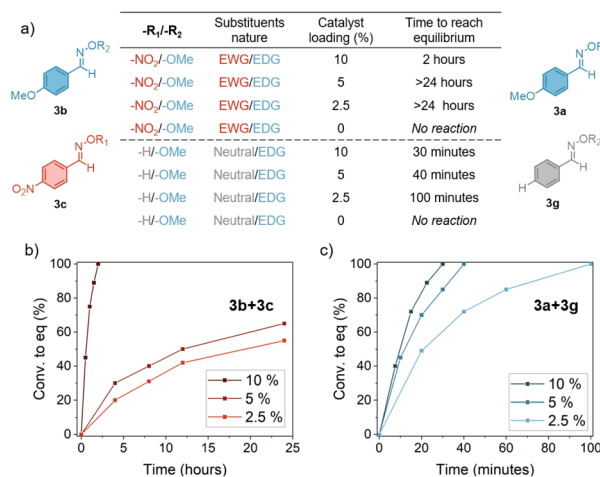Scheme 1 Chemical structures of the oxime-ethers synthesised in this work.

Fig. 2 (a) Summary of the catalyst loading screening for **3b/3c** and **3a/3g** oxime pairs. Kinetic plots of the metathesis reaction between (b) **3b** and **3c** (EDG-EWG) and (c) **3a** and **3g** (EDG-Neutral). *p*-TSA is used as catalyst. 100% conversion refers to point when equilibrium is reached and calculated from the integration of the ^{1}H-NMR peaks of the starting and product oxime protons.

10% of catalyst loading. We selected representative organocatalysts: 1,8-diazabicyclo[5.4.0]undec-7-ene (DBU) as a strong base, 1,5,7-triazabicyclo[4.4.0]dec-5-ene (TBD) as a dual nucleophile and base catalyst and *para*-toluene sulfonic acid (*p*TSA) as a strong acid. Methane sulfonic acid (MSA) was also included for two main reasons: (1) MSA is anhydrous whilst *p*TSA is monohydrate, so we could assess the influence of water in the reaction and (2) it has a similar pK_a as *p*TSA but is liquid which would ease their further inclusion in resin for the polymer synthesis.

The exchange reaction occurred only in the presence of strong acids. As a representative example, Fig. S1† shows the NMR spectra in the range 6.5–8.5 ppm recorded at 0, 15 and 120 minutes for the reaction between oxime **3b** and **3c**. At $t = 0$ min, the spectrum shows the characteristic singlets at 8.05 and 7.72 ppm of the oxime protons (–CH=N–O–) of the two starting oxime-ethers, **3b** and **3c**. As the reaction progressed, two new singlets appeared, at 8.11 and 7.66 ppm that are related to the new oxime-ethers formed, **3a** and **3d**. The reaction reached equilibrium after 120 minutes in the presence of 10% mol *p*-TSA. Notably, from the analysis of the complete ^{1}H-NMR spectra, only a small amount (<2% concerning the oxime-ethers) of the corresponding aldehydes could be identified, indicating that oxime-ethers are resistant to hydrolysis in the employed conditions. In the selected oxime pair (**3b**, bearing an electron donor group, EDG, and **3c** bearing an electron withdrawing group, EWG) equilibrium was reached after 2 h. When decreasing the catalyst loading to 5% or 2.5%, more than 24 h were needed to reach equilibrium, thus suggesting that the reaction kinetics have a strong acid dependence (Fig. 2). When considering a pair of oximes with different substituting groups (**3g**, bearing a neutral –H group, and **3a**, bearing an EDG), equilibrium was rapidly reached even at low acid concentrations, needing only 30 minutes in the case of 10% loading.

Given that equimolar reactions were run and that the presence of residual water or free oxime was negligible, these results indicated two main features: (i) the reaction takes place only in the presence of a strong acid catalyst and (ii) there is a significant substituent effect in the reaction kinetics. Due to the similarity between oxime and imine bonds, we initially hypothesised that the reaction must proceed *via* metathesis and could follow the same mechanism previously proposed for acid-catalysed imine metathesis (Fig. 3a, and Scheme S1†).[30,31] Hence, we considered hydrolysis or excess of free oxime to have a negligible impact in this study.

To support the above interpretation, we performed quantum chemical calculations (using B3LYP with a Def2-TZVP basis set and D3BJ dispersion correction) in the catalysed and non-catalysed model reactions. Fig. 3b reports the (ZPE corrected) Gibbs free energies as computed using the harmonic approximation and ideal gas thermodynamic statistics. The reaction proceeds through two transition states (TS1 and TS2) and one intermediate (INT). The relevant structures for the protonated system are highlighted in boxes. The reactants transform into the intermediate INT, passing through TS1. The energetic cost is attributed to the loss of the two double C=N bonds. The formation of the INT cyclic complex requires the formation of two new C–N bonds; their formation is not concerted although it takes place almost simultaneously and with no trace of additional minima in the potential energy surface.

The path from INT toward the products follows an analogous but reversed evolution. The overall thermodynamics of the reaction is essentially isoergonic and this feature is independent of the protonation state. Due to the ring strain of the 4-membered cycle, the cyclic intermediate INT is located at higher energies compared to both the reactants and the products. Its formation is destabilised by a significant negative entropic contribution due to the nature of the condensation reaction that brings its Gibbs free energy to 18 and 13 kcal mol^{-1} above the reactants for the neutral and protonated systems, respectively. In contrast with thermodynamics, the kinetics of the reaction are clearly influenced by the protonation state. In the neutral system, both barriers amount to nearly 70 kcal mol^{-1}, a situation that would render the reaction almost impossible, even under relatively energetic conditions. The weakening of the C=N provided by the protonation of one nitrogen is sufficient to bring both activation barriers down to slightly less than 30 kcal mol^{-1}, thus making the proton a very effective catalyst for the reaction.

Intrigued by the fast exchange observed in the model pair **3a**/**3g**, we extended the study to seven oxime pairs, as representatives of the different combinations of EWG, EDG and neutral substituent groups in the aromatic oximes. The results are summarised in Fig. 4, S2–S4.† We found that the exchange reaction kinetics varied substantially based on the nature of the substituents (from 30 min to 6 h to reach the equilibrium).

Notably, EDGs promoted faster exchange reactions (*i.e.* 30 min for **3f**/**3a** pair) while the presence of EWGs led to longer reaction times (**3d**/**3i** pair). We surmise that the changes in the kinetics may be related to the stabilisation of the rate-determining step of the proposed mechanism, which would
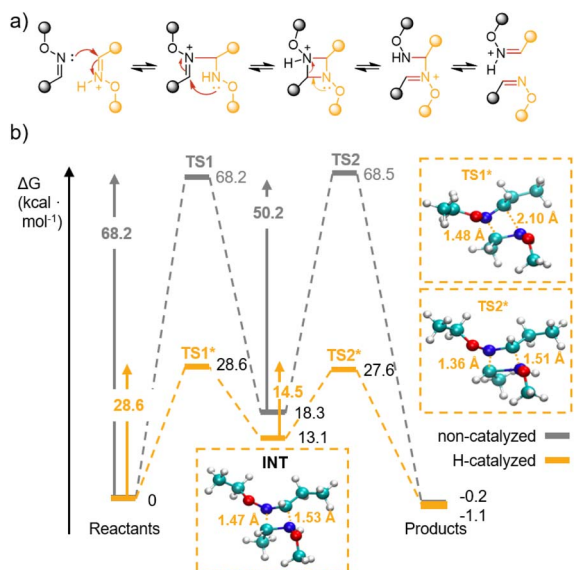

Fig. 3 (a) Proposed mechanism for the acid catalysed oxime metathesis studied herein. (b) Gibbs free energies (B3LYP-D3BJ/Def2-TZVP level) of the stationary points along the reactions path. The yellow lines and data correspond to the protonated pathway; the grey lines to the non-catalysed one. Insets correspond to the geometries of the TS1, INT and TS2 at the B3LYP/Def2-TZVP level of the protonated system.

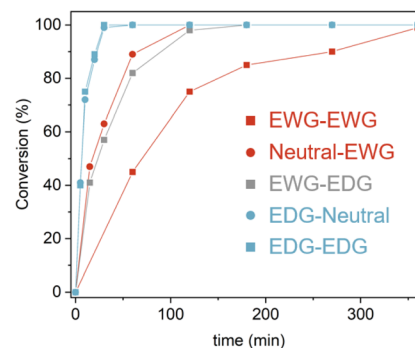| Oxime pair	-R$_1$	-R$_2$	Substituents nature	Time to reach equilibrium
3d/3i	-NO$_2$	-CF$_3$	EWG/EWG	6 hours
3d/3e	-NO$_2$	-CN	EWG/EWG	6 hours
3g/3d	-H	-NO$_2$	Neutral/EWG	2 hours
3a/3d	-OMe	-NO$_2$	EDG/EWG	2 hours
3g/3h	-H	-Cl	Neutral/EWG*	30 minutes
3g/3a	-H	-OMe	Neutral/EDG	30 minutes
3f/3a	-Me	-OMe	EDG/EDG	30 minutes

Fig. 4 Substituent effect study for the acid-catalysed oxime metathesis (10% *p*-TSA loading). (Top panel) Time required to reach equilibrium in the oxime metathesis reaction, depending on the substituents −R1 and R2 (*Halides are both EWG and EDG. Here we are considering EWG as predominant since it controls reactivity). (Bottom panel) Kinetic plot calculated from the integration of the ^{1}H-NMR peaks of the starting and product oxime protons. 100% conversion refers to point when equilibrium is reached.

imply the nucleophilic attack of the non-protonated oxime-ether by the protonated one (Scheme S2†). When –R1 is an EDG, the positive charge will be better stabilised, thus making the oxime-ether protonation easier. Moreover, an EDG on the non-protonated oxime-ether increases the nitrogen lone pair availability, making it more nucleophilic, thus facilitating the attack on the protonated oxime-ether. In contrast, an EWG hinders the oxime-ether protonation and also reduces the availability of the lone pair to act as a nucleophile, thus causing a drop in the reaction rate. To further explore these hypotheses, we conducted a computational study with two oxime couples (including EDG and EWG substituents and varying the initial protonation site) to determine the possible impact of substituents on the activation energies. The results, reported in Tables S1, S5–S8,† evidence a clear difference in the activation energies, with the EDG/EDG couple resulting in lower activation energy. Moreover, the obtained differences in activation energies are comparable with the reaction rate differences observed experimentally.

To exploit this dynamic system, we explored its implementation as the dynamic unit in a vitrimeric material. Hence, as a representative network, we achieved the cross-linking *via* a thiol–ene reaction using trimethylolpropane tris(3-mercaptopropionate) (TPTM), hexanedithiol (HDT) and the diallyl monomer **6a**, which contains the dynamic dioxime (Fig. 5a, see Methods†).[32] To confirm the stability of these dynamic bonds in the material, we assessed first the hydrolytic stability of the dioxime by ^{1}H NMR. Thus, **6a** was dissolved in a mixture of DMSO and water (8 : 2) with 5% of MSA and the mixture was heated at 70 °C for 16 h (Figure S9†). No change was observed in the NMR, detecting no aldehyde formation as a by-product. Conversely, an analogue imine was investigated (**7**) showing immediate hydrolysis upon dissolution in DMSO with 5% of MSA (Fig. S10†).

We attempted to study the network formation by means of FTIR, unfortunately, due to peak overlapping (SH stretch with oxime and aromatic C–H stretches), the thiol–ene reaction could not be tracked (Fig. S11a†). Nevertheless, we obtained an elastomeric material, with a T_g of −26 °C, as determined by DSC analysis (Fig. S14†) and a gel content of 94% (Soxhlet in THF).
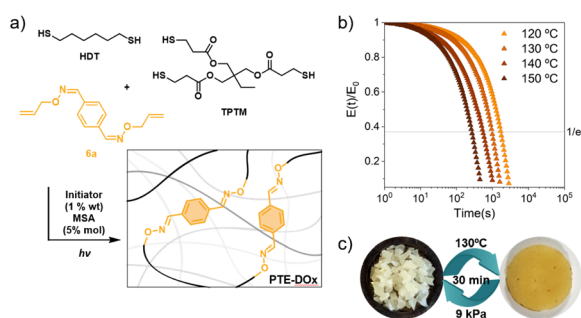
To prove the dynamic behaviour of the network, induced by the oxime metathesis, stress relaxation measurements in the linear viscoelastic regime were performed, applying a strain of 1% (Fig. 5b). The relaxation time (τ) was given by the point at which the stress of the samples relaxed to $1/e$ of their original stress. Full relaxation was observed and a linear regime is observed in the evaluated temperature range, as confirmed in the Arrhenius plot (Fig. 6b). In agreement with the molecular reactions, no stress relaxation was observed in the absence of MSA catalyst.

Also, the reprocessability of the PTE-DOx was tested by cutting it into small pieces and subjecting it to compression moulding at 130 °C for 30 minutes at 9 kPa (Fig. 5c). The reprocessed sample was characterised by FTIR and its rheological properties were tested by small amplitude oscillatory shear experiments in frequency sweeps, showing a plateau modulus close to the corresponding original material (Fig. 6c, orange, and S16†). As shown by ATR-FTIR, the reprocessed material showed no significant chemical change (Fig. S18a†).

To translate the substituent effect observed in the theoretical calculations and model reactions to the polymer network (faster oxime metathesis), a monomer bearing EDGs was included in the study. Thus, monomer **6b** was prepared from the corresponding methoxy-substituted terephtal-aldehyde, and the cross-linking of the network was achieved as depicted in Fig. 6a. Due to the high crystallinity of **6b** and hence poor solubility, only a network containing 20% mol of **6b** was achieved (PTE-DOx-OMe), since 50% content led to heterogeneous films and 100% was not able to crosslink (Fig. S14†). As for PTE-DOx, the obtained material, also showed elastomeric behaviour, exhibiting a T_g around −29 °C and a gel content of 92% (Fig. S14†).

As for PTE-DOx, the dynamic behaviour of the methoxy-containing network was evaluated through stress-relaxation experiments (Fig. S15†). Noticeably, as seen in the Arrhenius
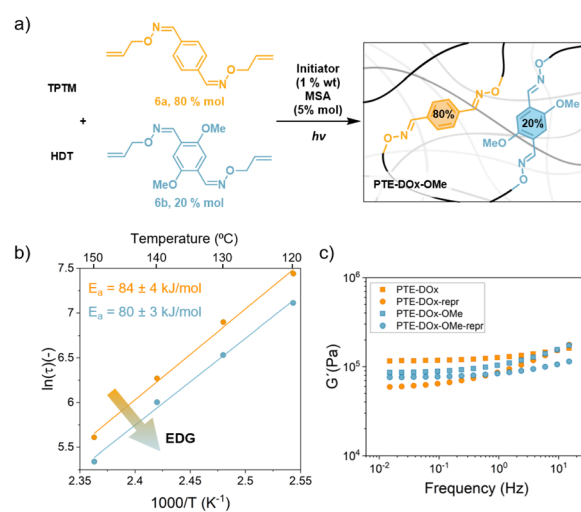

Fig. 5 (a) Chemical structures of monomers used for building the thioether–oxime network. (b) Normalised stress-relaxation curves of PTE-DOx at different temperatures. (c) Visual appearance of PTE-DOx before and after reprocessing under hot pressing at 130 °C and 9 kPa for 30 minutes.

Fig. 6 (a) Synthetic scheme for the synthesis of PTE-DOx-OMe network. (b) Arrhenius plot of the characteristic relaxation time of the dioxime materials and the corresponding activation energies. (c) G′ *vs.* frequency scans at room temperature for as-made and reprocessed materials.

plot (Fig. 6b), and in agreement with the model molecular reactions and supported by the DFT calculations, the electron donating substituent in the aromatic ring seems to accelerate the dynamic exchange in the polymer network, leading to faster relaxation times (*i.e.* ~400 s faster for PTE-DOx-OMe). Interestingly, the activation energy for both networks was similar (84 and 80 kJ mol^{-1}, respectively) suggesting that the substituent does not affect the temperature-dependent behavior of the material but it is clearly affecting the relaxation time.[33,34] Considering that we only have a 20% of methoxy-substituted oximes, these results seem consistent. Comparable behaviours have been observed in related thiol-yne crosslinked networks.[35]

PTE-DOx-OMe could be also reprocessed by hot pressing and the mechanical properties, evaluated by frequency sweep, are comparable with those found for the original material (Fig. S17 and S18†). Again, no chemical changes were noticed by means of FTIR (Fig. S19†).

Conclusions

Summarising, we have reported here the first example of an acid-catalysed oxime–metathesis reaction, performed between aromatic oxime–ethers. The proposed mechanism is supported by quantum chemistry studies that suggested the presence of a 4-membered cyclic intermediate and demonstrated the key role of the acidic catalyst. The study of the aromatic substituent effect on the oxime metathesis reaction rate highlighted how it can be easily tuned by changing the substituent; this experimental evidence is in line with the computational results. In addition, a model reaction involving a dioxime demonstrated its superior hydrolytic stability compared to the corresponding imine analogue. Finally, to show the applicability of this new reaction in the polymer field, two oxime-based CANs were prepared (PTE-DOx and PTE-DOx-OMe) and their dynamic character and reprocessability were demonstrated. The elastomeric materials were reprocessable showing comparable modulus to the virgin materials and the substituent effect in the polymer network was observed, agreeing with the faster relaxation times with the EDG-substitution in contrast to the EWG pairs. These features of the oxime metathesis reaction, together with the ease of oxime preparation and their resistance to side reactions (*i.e.* hydrolysis), make us believe that it will be a powerful tool in the field of DCC and dynamic networks.

Data availability

Raw experimental and computational data is available upon request to the corresponding author.

Author contributions

L. P. and H. S. conceived and initiated the study. L. P. and M. X synthesised the model compounds and the materials. E. B performed the theoretical calculations. G. V. and F. E. performed and supervised the rheological characterisation. F. L., E. B, M. X. and H. S. motivated and supervised the research program. L. P, M. X. and H. S. wrote a first draft of the

manuscript. All authors discussed the results and worked on the manuscript.

Conflicts of interest

There are no conflicts to declare.

Acknowledgements

References

1 S. J. Rowan, S. J. Cantrill, G. R. L. Cousins, J. K. M. Sanders and J. F. Stoddart, *Angew Chem. Int. Ed. Engl.*, 2002, **41**, 898–952.
2 S. Ulrich, *Acc. Chem. Res.*, 2019, **52**, 510–519.
3 J. Hu, S. K. Gupta, J. Ozdemir and H. Beyzavi, *ACS Appl. Nano Mater.*, 2020, **3**, 6239–6269.
4 Z. Lei, H. Chen, Y. Jin and W. Zhang, *Cell Rep. Phys. Sci.*, 2023, **4**, 101336.
5 C. J. Kloxin, T. F. Scott, B. J. Adzima and C. N. Bowman, *Macromolecules*, 2010, **43**, 2643–2653.
6 D. Montarnal, M. Capelot, F. Tournilhac and L. Leibler, *Science*, 2011, **334**, 965.
7 C. J. Kloxin and C. N. Bowman, *Chem. Soc. Rev.*, 2013, **42**, 7161–7173.
8 W. Denissen, J. M. Winne and F. E. D. Prez, *Chem. Sci.*, 2015, **7**, 30–38.
9 A. Kumar and L. A. Connal, *Macromol. Rapid Commun.*, 2023, **44**, 2200892.
10 F. Elizalde, R. H. Aguirresarobe, A. Gonzalez and H. Sardon, *Polym. Chem.*, 2020, **11**, 5386–5396.
11 A. Rekondo, R. Martin, A. R. de Luzuriaga, G. Cabañero, H. J. Grande and I. Odriozola, *Mater. Horiz.*, 2014, **1**, 237–240.
12 L. Li, X. Chen and J. M. Torkelson, *ACS Appl. Polym. Mater.*, 2020, **2**, 4658–4665.
13 P. Reutenauer, E. Buhler, P. J. Boul, S. J. Candau and J.-M. Lehn, *Chem.–Eur. J.*, 2009, **15**, 1893–1900.
14 A. Chao, I. Negulescu and D. Zhang, *Macromolecules*, 2016, **49**, 6277–6284.
15 M. E. Belowich and J. F. Stoddart, *Chem. Soc. Rev.*, 2012, **41**, 2003–2024.
16 P. Taynton, K. Yu, R. K. Shoemaker, Y. Jin, H. J. Qi and W. Zhang, *Adv. Mater.*, 2014, **26**, 3938–3942.

17 P. Taynton, C. Zhu, S. Loob, R. Shoemaker, J. Pritchard, Y. Jin and W. Zhang, *Polym. Chem.*, 2016, **7**, 7052–7056.

18 H. Li, J. Bai, Z. Shi and J. Yin, *Polymer*, 2016, **85**, 106–113.

19 J. Kalia and R. T. Raines, *Angew. Chem., Int. Ed.*, 2008, **47**, 7523–7526.

20 J. Collins, Z. Xiao, M. Müllner and L. A. Connal, *Polym. Chem.*, 2016, **7**, 3812–3826.

21 L. Shen, N. Cao, L. Tong, X. Zhang, G. Wu, T. Jiao, Q. Yin, J. Zhu, Y. Pan and H. Li, *Angew. Chem., Int. Ed.*, 2018, **57**, 16486–16490.

22 J. Collins, Z. Xiao and L. A. Connal, *J. Polym. Sci., Part A: Polym. Chem.*, 2017, **55**, 3826–3831.

23 G. N. Grover, J. Lam, T. H. Nguyen, T. Segura and H. D. Maynard, *Biomacromolecules*, 2012, **13**, 3013–3017.

24 S. Mukherjee, M. R. Hill and B. S. Sumerlin, *Soft Matter*, 2015, **11**, 6152–6161.

25 H. Sánchez-Morán, A. Ahmadi, B. Vogler and K.-H. Roh, *Biomacromolecules*, 2019, **20**, 4419–4429.

26 C. He, S. Shi, D. Wang, B. A. Helms and T. P. Russell, *J. Am. Chem. Soc.*, 2019, **141**, 13753–13757.

27 W.-X. Liu, C. Zhang, H. Zhang, N. Zhao, Z.-X. Yu and J. Xu, *J. Am. Chem. Soc.*, 2017, **139**, 8678–8684.

28 X. Chen, R. Wang, C. Cui, L. An, Q. Zhang, Y. Cheng and Y. Zhang, *Chem. Eng. J.*, 2022, **428**, 131212.

29 M. Ciaccia and S. D. Stefano, *Org. Biomol. Chem.*, 2014, **13**, 646–654.

30 G. Tóth, I. Pintér and A. Messmer, *Tetrahedron Lett.*, 1974, **15**, 735–738.

31 M. C. Burland, T. Y. Meyer and M.-H. Baik, *J. Org. Chem.*, 2004, **69**, 6173–6184.

32 K. F. Long, H. Wang, T. T. Dimos and C. N. Bowman, *Macromolecules*, 2021, **54**, 3093–3100.

33 B. Krishnakumar, R. V. S. P. Sanka, W. H. Binder, V. Parthasarthy, S. Rana and N. Karak, *Chem. Eng. J.*, 2020, **385**, 123820.

34 M. Guerre, C. Taplan, J. M. Winne and F. E. Du Prez, *Chem. Sci.*, 2020, **11**, 4855–4870.

35 N. Van Herck, D. Maes, K. Unal, M. Guerre, J. M. Winne and F. E. Du Prez, *Angew. Chem., Int. Ed.*, 2020, **59**, 3609–3617.